

Mechanical Properties of Solution-Processed Small-Molecule Semiconductor Films

Daniel Rodriquez,[†] Suchol Savagatrup,[†] Eduardo Valle,[†] Christopher M. Proctor,[‡] Caitlin McDowell,[‡] Guillermo C. Bazan,[‡] Thuc-Quyen Nguyen,[‡] and Darren J. Lipomi^{*,†}

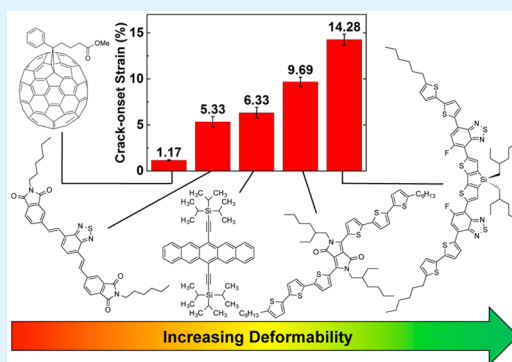
[†]Department of NanoEngineering, University of California—San Diego, 9500 Gilman Drive, Mail Code 0448, La Jolla, California 92093-0448, United States

[‡]Center for Polymers and Organic Solids, Department of Chemistry and Biochemistry, University of California—Santa Barbara, Santa Barbara, California 93106-9510, United States

S Supporting Information

ABSTRACT: Advantages of semiconducting small molecules—as opposed to semiconducting polymers—include synthetic simplicity, monodispersity, low cost, and ease of purification. One purported disadvantage of small-molecule films is reduced mechanical robustness. This paper measures the tensile modulus and crack-onset strain for pure films of the high-performance solution-processable small-molecule donors 7,7'-[4,4-bis(2-ethylhexyl)-4H-silolo[3,2-b:4,5-b']dithiophene-2,6-diyl]bis[6-fluoro-4-(5'-hexyl-[2,2'-bithiophen]-5-yl)benzo[c][1,2,5]thiadiazole] (DTS(FBTTh₂)₂), 2,5-di(2-ethylhexyl)-3,6-bis(5''-n-hexyl-[2,2',5',2'']-terthiophen-5-yl)-pyrrole[3,4-c]pyrrole-1,4-dione (SMDPPEH), and 6,13-bis(triisopropylsilyl)ethynylpentacene (TIPS-pentacene), the acceptor 5,5'-(2,1,3-benzothiadiazole-4,7-diyl)-2,1-ethenediyl]bis[2-hexyl-1H-isoindole-1,3(2H)-dione] (HPI-BT), blends of DTS(FBTTh₂)₂ and SMDPPEH with [6,6]-phenyl C₇₁ butyric acid methyl ester (PC₇₁BM) and with HPI-BT, and bulk heterojunction films processed with the additives 1,8-diiodooctane (DIO) and polystyrene (PS). The most deformable films of solution-processed organic semiconductors are found to exhibit tensile moduli and crack-onset strains comparable to those measured for conjugated polymers. For example, the tensile modulus of as-cast DTS(FBTTh₂)₂ is 0.68 GPa (i.e., comparable to poly(3-hexylthiophene) (P3HT), the common polymer), while it exhibits no cracks when stretched on an elastomeric substrate to strains of 14%. While this high degree of stretchability is lost upon the addition of PC₇₁BM (4.2 GPa, 1.42%), it can be partially recovered using processing additives. Tensile modulus and crack-onset strain are highly correlated, which is typical of van der Waals solids. Increased surface roughness was correlated to increased modulus and brittleness within films of similar composition. Decreased stiffness for soluble molecular semiconductors can be rationalized by the presence of alkyl side chains, which decrease the van der Waals attraction between molecules in the crystalline grains. These measurements and observations could have important consequences for the stability of devices based on molecular semiconductors, especially those destined for stretchable or ultraflexible applications, or those demanding mechanical robustness during roll-to-roll fabrication or use in the outdoor environment.

KEYWORDS: organic semiconductors, small molecules, additives, stretchable electronics, mechanical properties, organic solar cells



INTRODUCTION

Organic semiconductors fall into two categories: polymers and small molecules. While both classes of materials have achieved similar levels of performance in thin-film transistors (i.e., charge-carrier mobility) and solar cells (i.e., efficiency), each class of material has its own set of advantages and disadvantages.¹ For example, polymers can be easier to coat from solution than are small molecules.² Small molecules, however, are by definition monodisperse and thus less subject to batch-to-batch variability.³ One advantage typically posited for polymers is superior mechanical resilience compared to that of small molecules, because small molecules are van der Waals solids that do not have entanglements and thus increased

strength and toughness, which are characteristic of polymeric materials.⁴ It is thus granted that the total energy that can be absorbed by conjugated polymers in either the elastic or plastic regimes of deformation—as manifested in the resilience, tensile strength, and toughness—will almost certainly surpass that of small-molecule semiconductors. The ability to store or dissipate significant mechanical energy, however, may be irrelevant in an encapsulated module, where the resistance to deformation is provided by the substrate. Thus, low tensile modulus (to reduce

Received: March 1, 2016

Accepted: April 19, 2016

Published: April 19, 2016

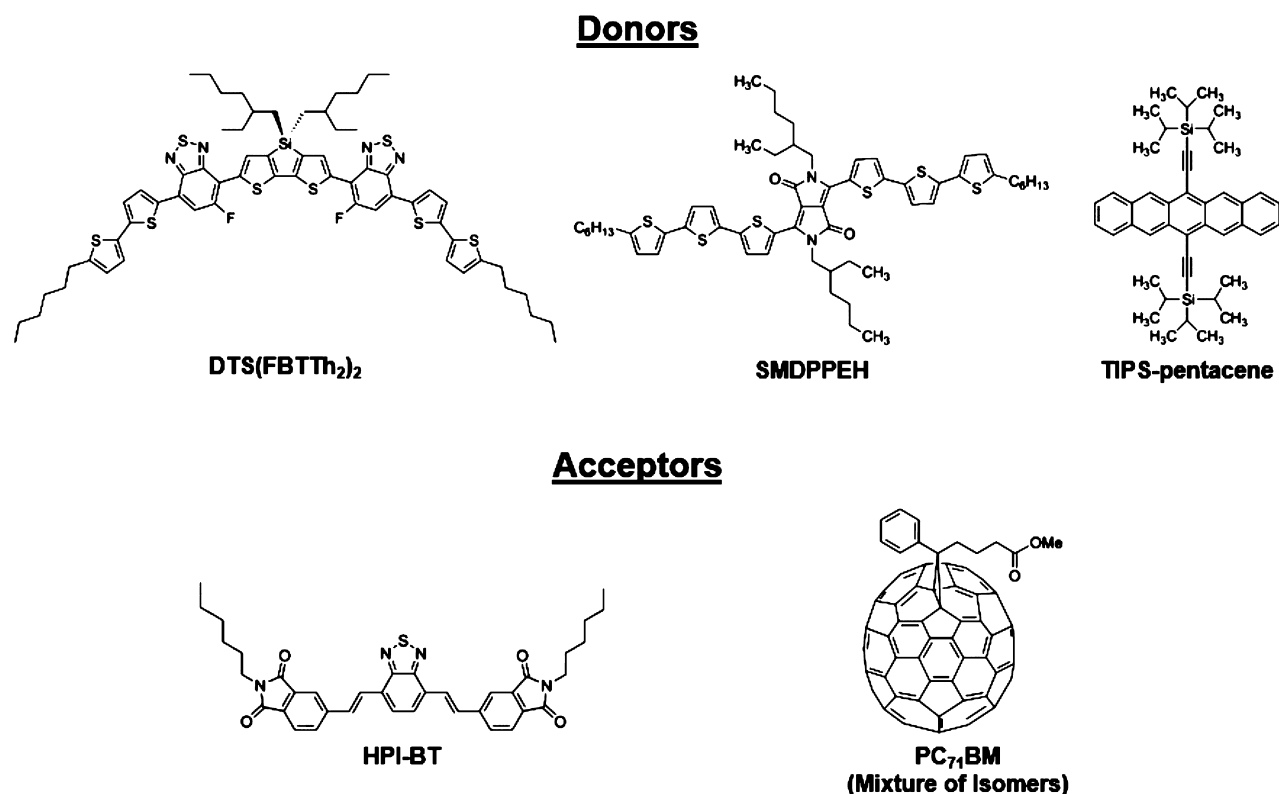


Figure 1. Chemical structures of the small molecules whose mechanical properties were measured in this work. Mechanical properties of DTS(FBTTh₂)₂, SMDPPEH, TIPS-pentacene, and HPI-BT were measured for the first time, while those of PC₇₁BM were first reported in ref 5.

interfacial stresses upon bending or tensile deformations) and high strains at which the first cracks appear may be the most relevant predictors of the lifetime of organic electronic devices, at least for bending and stretching deformations. Despite the importance of mechanical properties in determining the lifetime and range of application of flexible (or even stretchable) organic electronic devices, tensile modulus and crack-onset strain have never been reported for solution-processed small-molecule semiconductors. This paper reports these quantities for the first time for four of the five materials (PC₇₁BM has been reported previously)⁵—three electron donors and one acceptor (Figure 1)—which are promising for thin-film transistors when used alone, or for solar cells when mixed with PC₇₁BM or other acceptors.

Devices based on organic semiconductors—e.g., solar cells, thin-film transistors, light-emitting devices, and RFID tags—have the potential to be fabricated by gravure, screen, slot-die, and inkjet printing in roll-to-roll modalities, and thus may have advantages to traditional devices based on silicon for applications demanding low-cost.⁶ These low-cost (and sometimes short-lived) devices for which organic materials are regarded as the ideal solutions (e.g., for portable and disposable applications) are often made on flexible foils and must survive mechanical forces during both fabrication and use.⁷ Despite mechanically demanding form factors for thin-film organic electronic devices, the electronic properties of such devices are nearly always optimized on glass or silicon substrates, and thus the mechanical properties that will affect the lifetime in the real world are not known and seldom tested. The absence of mechanical information on these compounds is salient because the cohesive fracture energies of these materials, generally within the range of 1–10 J m^{−2}, are a few orders of magnitude

smaller than those of conventional semiconductors and engineering plastics.⁸ While the deformability of one class of solution-processed organic semiconductor—conjugated polymers—is generally regarded as favorable, our work and that of others has revealed that these materials occupy a wide range of mechanical behavior that depends crucially on molecular and solid-state packing structure.^{9–13} In contrast, the deformability of small-molecule semiconductors is generally purported to be unfavorable.

We reasoned that the payoff, in the event that our experiments were to reveal unexpectedly high deformability in small-molecule films, would be significant. At the outset, however, we had reason to doubt such a favorable outcome, as pentacene—albeit without an alkyl chain—was found by Tchk and co-workers to have a tensile modulus of 16 GPa (an order of magnitude stiffer than P3HT) and crack at compressive strains (probably significantly) less than 4% on elastomeric substrates (tensile strains were not tested, but it is expected to fracture at small strains).¹⁴ Moreover, our laboratory previously found that films of PC₆₁BM and PC₇₁BM crack at <0.5% tensile strains on elastomeric substrates.⁵ Unsubstituted small molecules deposited by vacuum deposition (e.g., pentacene) and those containing a low fraction of aliphatic carbon atoms compared to π -conjugated atoms (e.g., methanofullerenes), however, are not representative of state-of-the-art soluble small-molecule semiconductors, which contain relatively long or branched alkyl chains.¹⁵

Mechanical Properties of van der Waals Solids. In considering the mechanical properties of small-molecule organic semiconductors, it is worth considering the mechanical response of polymeric semiconductors, about which more is known. For a semicrystalline conjugated polymer, tensile

deformation in the elastic regime is accommodated principally by straightening of the chains in the amorphous domains; the loss in entropy produces a restoring force. To the extent that the crystalline domains deform elastically, strain energy is stored in the van der Waals bonds being shifted from equilibrium; compressive strains are resisted by steric repulsive forces and tensile strains are resisted by attractive van der Waals forces between the molecules in the solids. For conjugated polymers, structures that form highly crystalline microstructures due to fused rings in the backbone, interdigitation of the side chains, or both, exhibit increased stiffness.^{16,17} When the semicrystalline polymer plastically deforms—i.e., when the yield point is surpassed—the strain energy is absorbed by crystallization of aligned chains in the amorphous domains, rearrangement of the van der Waals bonds in the crystalline domains, and the formation of crystallites that are partially aligned along the stretched axis, and which exhibit birefringence.¹⁸ Finally, decohesion and fracture occurs by pullout of chains and by scission of covalent bonds.⁸

For small-molecule semiconductors, most of the modes by which strain energy is stored or absorbed that are characteristic of polymers are absent. Solution-processed small-molecule semiconductors can be glassy, polycrystalline, or semicrystalline, and thermal annealing tends to increase the average size of the crystallites if the molecules can crystallize.¹⁹ In the case of glassy semiconductors such as di(4-methylphenyl)methano- C_{60} bis-adduct (DMPCBA), the film remains amorphous upon deposition and (up to 20 h) after thermal annealing.²⁰ The glassy nature and thermal stability of this material is a result of its chemical structure which sterically prevents the C_{60} cores from close packing, rendering it soluble but amorphous in the solid state.²⁰ Thus, the energy of elastic deformation is stored solely by perturbation of the molecules in the glass, and the elastic modulus is determined by the strength of the van der Waals bonds. The strength of these bonds is lowered by the presence of side chains (which push the polarizable cores of the molecules farther from each other) and branching in the side chains. The sizes of core structures that have similar rigidities have a relatively small stiffening effect on the solid material, as solid anthracene is only slightly stiffer than naphthalene (8.4 vs 8.1 GPa).²¹ The presence of a flexible group in the core reduces the stiffness, however, as the modulus of solid diphenylethane is 6.3 GPa.²¹ Possible mechanisms of plastic deformation include deformation of the crystallites that retain the same lattice structure, or hypothetically by the formation of strained crystalline polymorphs.²²

■ EXPERIMENTAL DESIGN

Selection of Materials. The overall goal of this study was to correlate the chemical structures of small molecules to their thin film mechanical properties and to elucidate the necessary features for mechanical deformability. To this end, we measured the properties of four different molecular semiconductors: DTS(FBTTh₂)₂, SMDPPEH, and TIPS-pentacene (donors), and HPI-BT (an acceptor), whose structures are shown in Figure 1. To measure the properties of films relevant to organic solar cells, we also measured the mechanical properties of DTS(FBTTh₂)₂ and SMDPPEH in bulk heterojunctions with HPI-BT, and with the standard electron acceptor, PC₇₁BM. DTS(FBTTh₂)₂ is an example of a high-performance organic semiconductor that has achieved power conversion efficiency (PCE) of up to 7%, when mixed with PC₇₁BM and 0.4% DIO in the active layer.²³ This performance

exceeds that of the highest performing solar cells comprising active layers of P3HT and PC₆₁BM. TIPS-pentacene was selected because the mechanical properties of the core structure, pentacene, were measured by Tahk et al.,¹⁴ and thus this material provides a comparison between an unsubstituted core structure, and a structure bearing side chains. DTS(FBTTh₂)₂ is a high-performance donor for organic solar cells.²³ The crystal structure of DTS(FBTTh₂)₂ is triclinic with two molecules assigned to a unit cell, and exhibits alkyl stacking, hexyl stacking, and π – π overlap.³ Upon thermal annealing, crystallites in the as-cast film grow into large fibrils and form highly ordered regions that exhibit lamellar stacking. SMDPPEH was selected for its relatively simple chemical structure, and the ubiquity of the DPP group as an electron-deficient unit in low-bandgap molecular and polymeric semiconductors. SMDPPEH has achieved PCE values of up to 3% with PC₇₁BM as the acceptor.²⁴ PC₇₁BM is the standard acceptor in high-performance organic solar cells. We have measured its modulus and crack-onset strain in a previous publication and found that “technical grades” of PC₇₁BM—which comprise a mixture of incompletely separated but otherwise pure derivatives of C_{60} and C_{70} in which $\geq 90\%$ of the blend is PC₇₁BM—are more elastic and ductile than pure films of either PC₆₁BM or PC₇₁BM.⁵ Moreover, compared to PC₆₁BM, PC₇₁BM has the greater deformability, most likely because of its existence as a mixture of isomers and therefore decreased tendency to form well packed structures in the solid state.⁵ Because of the high cost and production energy of fullerene derivatives,²⁵ the community has been seeking nonfullerene electron acceptors.²⁶ One such example is HPI-BT, whose mechanical properties we also tested in this work.

Selection of Processing Additives. Processing additives are ubiquitous in high-performance organic solar cells.²⁷ For example, the presence of 1,8-diiodooctane (DIO) significantly increases the PCE of cells based on DTS(FBTTh₂)₂:PC₇₁BM bulk heterojunctions: from 5.8% to 7.1% when mixed with a solution containing 0.4% DIO by volume.³ Another class of additives is polymeric. For example, high molecular weight polystyrene (PS) has been shown to increase PCE values further, from 7.1% to 8.2% by adding 2.5 wt % ($M_n = 20$ MDa).² Addition of PS improves wetting, increases thickness and absorbance, and leads to a morphology consisting of large interpenetrated fibrils, as seen in bright-field TEM images.² We hypothesized that both DIO and PS ($M_n = 900$ kDa and 20 MDa) might increase the mechanical compliance and ductility of devices based on small-molecule semiconductors, in particular DTS(FBTTh₂)₂:PC₇₁BM bulk heterojunction films.

Mechanical Characterization: Tensile Modulus. The tensile modulus of a solid is the slope of a plot of stress vs strain in the elastic (linear, low-strain) regime of deformation. It describes the ability of a solid to store potential energy due to a load, or its tendency to resist elastic deformation. It is one of the many manifestations of the strength of the intermolecular forces in a van der Waals solid. We measured the tensile modulus using the well-known buckling-based metrology (i.e., surface wrinkling).²⁸ This method is a well-established quantitative and rapid method of analyzing the mechanical properties of thin film systems such as organic semiconductors, polymer brushes, and nanoscale structured materials whose mechanical properties can be otherwise difficult to measure.²⁸ Measurements produced from this method agree well with those obtained from traditional pull testing—when sufficient quantities of the material are available for conventional

measurements—and dynamic mechanical analysis.²⁹ We suggest that the low tensile modulus is possibly desirable for mechanically robust thin films because it reduces interfacial stresses with load-bearing substrates and encapsulants. Moreover, for semiconducting polymers with relatively low molecular weight tested in the literature so far, low tensile modulus is often correlated with high ductility (crack-onset strain).⁵

Mechanical Characterization: Crack-Onset Strain. The crack-onset strain of a thin film on an elastic substrate is an indirect measurement of the strain at fracture, which is—like the buckling technique for measuring the tensile modulus—useful if not enough material is available for conventional tensile testing. The method is indirect because it is dependent on the adhesion between the film and the substrate (poor adhesion localizes strain to thin areas and defects in the film, and thus leads to increased effective brittleness).²⁹ Nevertheless, it is a useful metric for comparison between similar materials of their respective abilities to accommodate strain without fracture. Two different methods of determining the crack-onset strain were employed: stretch tests (high-strain regime, Figure 2a) and bending tests (low-strain regime, Figure

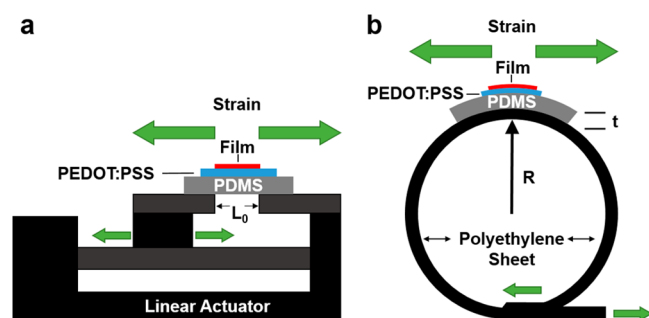


Figure 2. Schematic diagram of the two methods of determining crack-onset strain. (a) Stretch test (high-strain regime). (b) Bending test (low-strain regime).

2b). Stretch tests were employed as a quick and effective means of determining the crack-onset of films that can be strained $>5\%$ (high-strain regime). The strain (ϵ) induced in the stretch test was calculated using $\Delta L/L_0$, where L_0 is the original length, and ΔL is the change in length. We used bending tests to access lower strains of especially brittle materials, for which stretch tests could not resolve the crack-onset strain.³⁰ The bending test offers precise control over the applied strain, either by varying the thickness t or the radius of curvature R , $\epsilon = t/R$, and could be used to access strains of 0.5% to 15%, but was most useful for materials that fractured at small strains, 0.5% to 2%.

RESULTS AND DISCUSSION

General Observations. Values of tensile modulus (top row, blue) and crack-onset strain (bottom row, red) are shown in Figure 3. The strong correlation between these quantities is shown in Figure 4. Five key observations can be made. (I) The nonfullerene small-molecules DTS(FBTTh₂)₂, SMDPPEH, TIPS-pentacene, and HPI-BT are substantially more compliant (modulus <1.5 GPa) and stretchable (crack-onset strain $>5\%$) compared to the modulus and brittleness measured previously for other small molecular semiconductors, including methanofullerenes⁵ or unsubstituted pentacene.¹⁴ In particular, DTS(FBTTh₂)₂ had the lowest tensile modulus of the pure small-molecule films (0.79 GPa) and could absorb the greatest

strain before failure, up to 14%. (II) The bulk heterojunction films comprising DTS(FBTTh₂)₂ or SMDPPEH and PC₇₁BM were significantly stiffer and more brittle than pure films of the small molecular donors. This observation is consistent with the stiffening effect of methanofullerenes on conjugated polymers in general: for poly(3-alkylthiophene)s (P3ATs), PC₆₁BM behaves as an antiplasticizer.^{5,31} (III) Annealing bulk heterojunction films of DTS(FBTTh₂)₂:PC₇₁BM increases the tensile modulus from 4.2 to 17.6 GPa and decreases the crack-onset strain from 1.4% to 1.1%. (IV) The effect of the additives DIO and PS on bulk heterojunction films of DTS(FBTTh₂)₂:PC₇₁BM is to decrease the tensile modulus and increase the crack-onset strain. (V) Bulk heterojunction films of the two molecular donors with the acceptor HPI-BT are significantly more deformable than the same donors mixed with PC₇₁BM. Observations *I–V* will be examined in detail below.

I. Softening Effect of Side Chains. The effect of side chains on comb-like polymers is, in general, to reduce the glass transition temperature, modulus, brittleness, and tensile strength.³² This effect is well-known in P3ATs, (semiconducting polymers for which the rationale for the softening effect of side chains in polymers is that side chains reduce the density of load-bearing covalent bonds along the strained axis and reduce the density of noncovalent interactions between main chains).²⁹ To find the glass transition temperature, T_g , of the small molecules under study, we conducted differential scanning calorimetry (DSC) measurements, however, no clear T_g was observed in any of the materials (Figure S2 of the Supporting Information, SI). The lack of an observable T_g from DSC thermograms of similar materials has been reported by others and complementary measurements such as modulated-temperature DSC (MTDSC) are usually required to observe the glass transition.³³ To elucidate the affect of side chains in small-molecule semiconductors, we compared the tensile modulus of TIPS-pentacene, 2.95 ± 0.36 GPa, to the modulus of unsubstituted pentacene films measured by Tahk et al. using the buckling technique, 16.09 ± 2.83 GPa.¹⁴ The softening effect of side chains was investigated in molecular monolayers by Cun et al. in a study of *N,N'*-dihexadecyl-quinacridone (QA16C). This molecule possesses two alkyl side chains that are each 16 carbon atoms long but has a core that is isosteric with pentacene.³⁴ The authors used both STM measurements and density functional theory (DFT) calculations, which predicted a tensile modulus of 0.92 ± 0.08 GPa.³⁴ The analysis of the authors suggested that the origin of the elastic properties of QA16C arose due to conformational changes in the side chains under mechanical strain.³⁴

II. Stiffening and Embrittling Effect of PC₇₁BM. Similar to its effect on the mechanical properties of conjugated polymers, PC₇₁BM was observed to stiffen and embrittle bulk heterojunction films in which the donor is a small molecule (Figure 3c and d). For example, the tensile modulus of DTS(FBTTh₂)₂ was increased by a factor of 5 in the bulk heterojunction, and its crack-onset strain was decreased by a factor of 10. For P3AT: methanofullerene bulk heterojunction films comprising a crystalline P3AT phase, a fullerene-rich phase, and an amorphous mixed phase, the fullerene increased the glass transition temperature of the mixed phase.⁵ Moreover, the mechanical properties of the fullerene-rich phase were thus dominated by the properties of the fullerene, which was stiff and brittle.⁵ For small-molecule:fullerene bulk heterojunction films, we postulate similar effects. The microstructure of as-cast SMDPPEH:PC₇₁BM does not exhibit large phase separation,

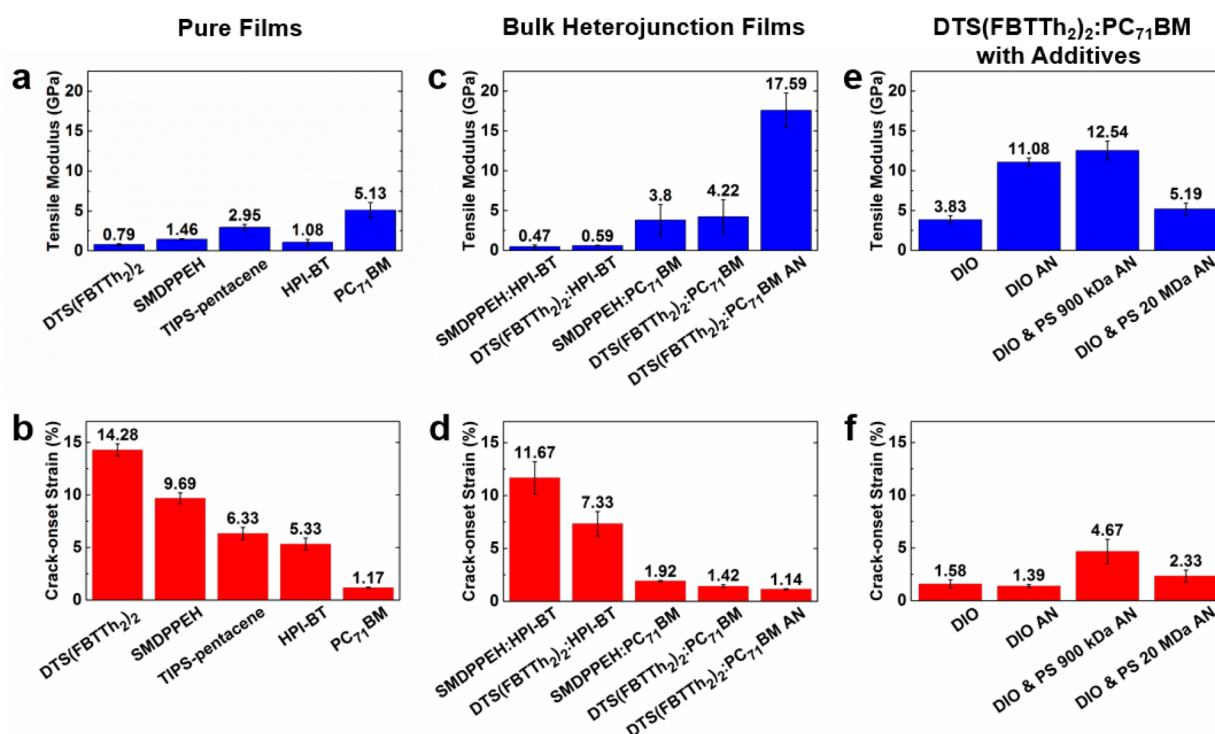


Figure 3. Tensile modulus of pure small-molecule thin films (a) mixed bulk heterojunction thin films (b) and films containing additives (c). Crack-onset of pure small-molecule thin films (d), mixed bulk heterojunction thin films (e), and films containing additives (f).

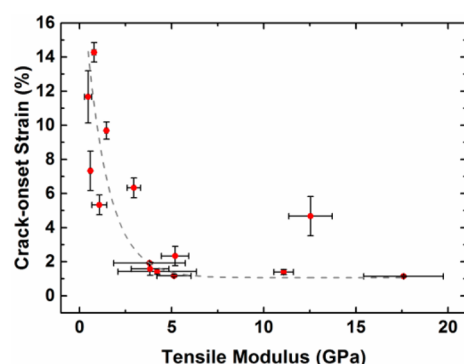


Figure 4. Correlation between tensile moduli and crack-onset strains for all the films tested.

but consists of fiberlike structures, SMDPPEH rich domains, and oval-shaped features attributed to PC₇₁BM-rich domains.²⁴ Morphological features in the films were differentiated by decreasing the donor to acceptor ratio and observing that the oval features grew in size with increasing PC₇₁BM concentration.²⁴ A structural analog, DPP(TBFu)₂—in which the terminal alkylated bithiophene units of SMDPPEH are replaced with benzofuran units—has also been reported. DPP(TBFu)₂:PC₇₁BM is well mixed and amorphous when as cast with no thermal treatment. Upon annealing, DPP(TBFu)₂ nuclei were found to grow and expel PC₇₁BM; separation of phases was found to create a DPP(TBFu)₂ rich phase consisting mainly of crystallites, along with a PC₇₁BM-rich phase.³⁵

III. Increased Stiffness and Brittleness by Thermal Annealing. Thermal annealing had a profound increase on the modulus of DTS(FBTTh₂)₂:PC₇₁BM films, blended in a weight ratio of 3:2, (from 4.2 to 17.6 GPa) and increase in brittleness (crack-onset strain from 1.42% as-cast to 1.14%

annealed). We chose this system for thermal annealing because this treatment was included in the procedure that produced the best solar cells from these materials,²³ but in all polymers, small-molecules, and bulk heterojunction films we have ever measured, we have never observed an organic semiconductor film to soften when thermally annealed.³⁶ The stiffening effect can be correlated to microstructural features observed previously: when mixed with PC₇₁BM, the as-cast DTS(FBTTh₂)₂:PC₇₁BM bulk heterojunction film was found to be largely well mixed and amorphous.³ As the film is annealed, DTS(FBTTh₂)₂ crystallizes into wire-like structures and PC₇₁BM-rich domains.³ A similar stiffening effect has been observed in polymeric systems after thermal annealing, for example PBTtT.¹⁷ O'Connor et al. measured the tensile modulus of as-cast and annealed PBTtT thin films and reported moduli of 0.88 ± 0.24 and 1.8 ± 0.35 GPa, respectively, an order of magnitude stiffer.¹⁷ They attributed the large increase in modulus to changes in microstructural features: an increase in overall crystallinity and an increase in the size of the crystallites.¹⁷

IV. Effect of Additives. Processing additives offer a means of improving device functionality without the need for extra processing steps, such as thermal or solvent annealing.³⁷ Their function can vary, but under favorable circumstances, they help to achieve a solid-state microstructure that augments charge separation compared to an unmodified bulk heterojunction film.³⁷ In a previous paper, we reported a plasticizing effect of both DIO and low-molecular-weight PDMS on P3HT:PC₆₁BM bulk heterojunction films.²⁹ A similar plasticizing effect of both DIO and polystyrene of 900 kDa and 20 MDa molecular weight on the mechanical properties of DTS(FBTTh₂)₂:PC₇₁BM is shown in Figure 3e and f. The microstructure of DTS(FBTTh₂)₂:PC₇₁BM:DIO has been found to have more phase separation compared with

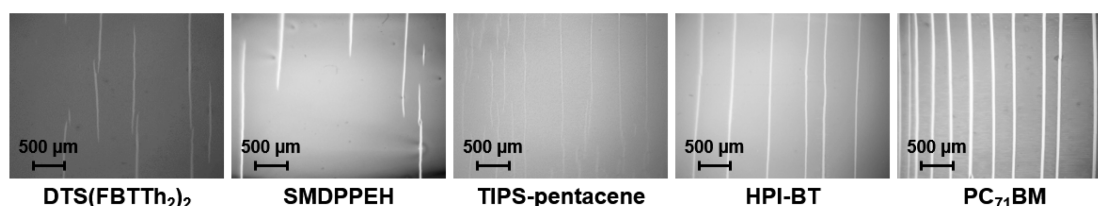


Figure 5. Optical micrographs of cracking behavior of four pure organic semiconductors at 15% strain, from partially brittle behavior (left) to completely brittle behavior (right).

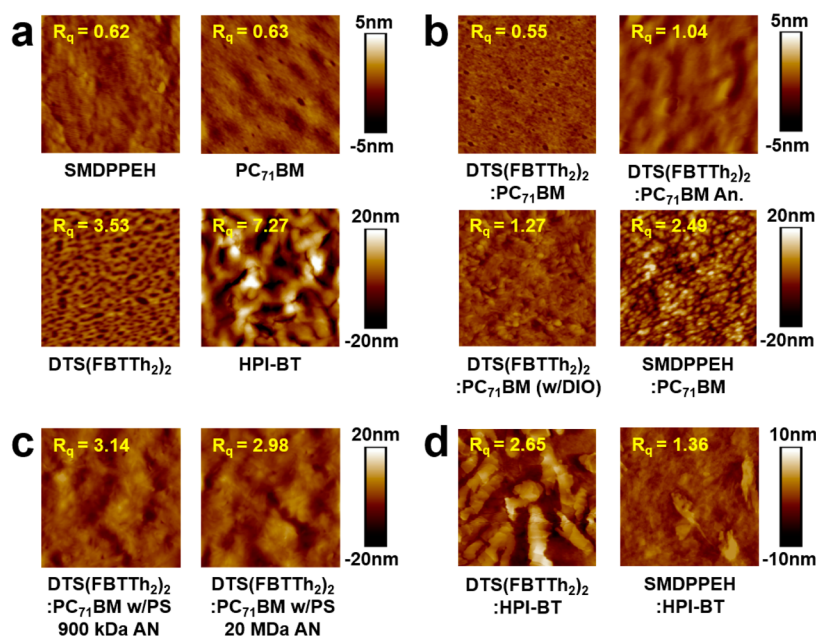


Figure 6. Surface morphology of thin film bulk heterojunction solar cells. (a) Pure small-molecule donor and acceptor thin films. (b) Small-molecule bulk heterojunction thin films mixed with PC₇₁BM. (c) DTS(FBTTh₂)₂:PC₇₁BM bulk heterojunction films with 900 kDa and 20 MDa polystyrene additives, after thermal annealing. (d) Small-molecule bulk heterojunction thin films mixed with HPI-BT.

DTS(FBTTh₂)₂:PC₇₁BM and also exhibits larger grains.³⁸ When PS was added to the bulk heterojunction, the microstructure of DTS(FBTTh₂)₂:PC₇₁BM:DIO:PS evolved into one with long DTS(FBTTh₂)₂ fibrils, well-mixed domains, and PS-rich domains.³⁸ The DTS(FBTTh₂)₂ fibrils crossed PS-rich domains that were well dispersed throughout the film. It may be possible that the PS-rich domains serve to accommodate strain when the film is under tension, which would be consistent with the observed increase in crack-onset, from 1.58% to 4.67%, with the addition of PS. All of these additives produced significant reductions in the tensile modulus and increase in the crack-onset strain. Given that these additives can also increase the PCE of organic solar cells, it seems that the use of additives might be one approach to achieving the “best of both worlds” of electronic performance and mechanical deformability.

V. Mechanical Properties of Bulk Heterojunctions with HPI-BT as the Acceptor. Given the well-known stiffening effect of fullerenes on bulk heterojunctions comprising either a conjugated polymer or small molecule as the donor, a substitute for the fullerene with greater deformability would be beneficial. We observed that the small-molecule HPI-BT was a factor of 5 more compliant than PC₇₁BM, and also a factor of 5 more ductile (Figure 3a and b). Moreover, bulk heterojunctions comprising DTS(FBTTh₂)₂:HPI-BT and SMDPPEH:HPI-BT were both significantly more deformable than bulk heterojunctions in which the acceptor was PC₇₁BM (Figure 3c and d).

Since the bulk heterojunction consisted of only nonfullerene small molecules and exhibited a relatively large degree of stretchability, we fabricated organic solar cells comprising only stretchable components, including an anode containing highly plasticized poly(3,4-ethylenedioxythiophene):poly(styrenesulfonate) (PEDOT:PSS) and a cathode of liquid eutectic gallium indium, although the efficiencies were very low for this pair of materials (Figure S1).

Mode of Fracture. The way in which organic thin films fracture under strain has important technological consequences. For ductile fracture, in which cracks open but do not span the entire width of the film perpendicular to the strained axis, it should still be possible to use these materials in devices requiring lateral charge transport (i.e., thin-film transistors). For materials exhibiting brittle fracture, in which cracks easily propagate across the entire dimension perpendicular to the strained axis, devices with lateral charge transport will likely be inoperable. The type of fracture observed was qualitatively related to the crack-onset strain (Figure 5). That is, materials with small crack-onset strains exhibited brittle fracture.

Correlation of Surface Morphology with Mechanical Properties. For small-molecule films, we found that the surface roughness was a strong predictor of the stiffness within films of the same composition, but not between films of different compositions (Figure 6). For example, in the case of DTS(FBTTh₂)₂, pure films are rough (RMS roughness 3.53 nm) compared with SMDPPEH (0.62 nm), but DTS-

(FBTTh₂)₂ exhibits a lower modulus. Thermal annealing of DTS(FBTTh₂)₂ doubled the RMS roughness to 6.92 nm; this increase was consistent with the growth of crystals in the film. However, addition of PC₇₁BM produced a smoother film (RMS roughness of 0.55 nm), but the modulus increased substantially, as PC₇₁BM may interrupt some of the ordering seen in the pure film. Upon thermal annealing, the RMS roughness doubled to 1.04 nm; this increase in roughness was accompanied by a large increase in tensile modulus from 4.22 to 17.59 GPa. Our results were consistent with those observed in P3ATs, which exhibited an increase in surface roughness that correlated to an increase in tensile moduli as the alkyl side chains became shorter.²⁹ This trend was attributed to an increased degree of crystallinity within films containing shorter alkyl chains for P3ATs, and thus increased tensile modulus.²⁹

Mechanism of Strain Accommodation in Small-Molecule Films. As we hypothesized, alkyl-substituted, solution-processable small molecules indeed possess greater deformability than unsubstituted π -conjugated small molecules (e.g., acenes). Alkyl solubilizing groups separate the conjugated core units from each other, and thus reduce the van der Waals cohesive energy. Accordingly, the interplanar distance in SMDPPEH was found to be 1.47 nm by grazing-incidence X-ray diffraction.¹⁹ In contrast, the spacing in DTS(FBTTh₂)₂ was 2.2 nm in the (001) direction, which describes the stacking of ethylhexyl side chains of the dithienosilole unit spaced between conjugated backbones, and 1.6 nm in the (011) plane which corresponds to the end-capped hexyl stacking.³ In either direction, the spacing in SMDPPEH was found to be smaller than in DTS(FBTTh₂)₂, suggesting stronger intermolecular forces and possibly higher tensile modulus (although the mechanical trends were uncorrelated to melting transitions observed by DSC, Figure S2). The crack-onset strains of DTS(FBTTh₂)₂ and SMDPPEH in particular were greater than or approximately equal to 10%. This high degree of stretchability could be accommodated by plastic deformation of the crystalline grains themselves, though ultraviolet–visible spectroscopy (Figure S3) revealed only minor differences in absorption between pristine films and those stretched to 10%, and thus did not indicate significant evolution in the microstructure, except for a broadening and red-shifted onset of the absorption for SMDPPEH. Molecular modeling and in situ X-ray diffraction during the process of deformation could yield insights regarding the mechanism of plastic deformation in these and similar materials.

CONCLUSIONS

Our examination of the mechanical properties of high-performance organic semiconductors revealed unexpected deformability—low tensile modulus and high crack-onset strain—of solution-processable small molecules. These findings suggest that devices employing pure films of organic semiconductors, e.g., for thin-film transistors, could be subjected to significant deformations without mechanical failure. For solar cells, in which the donors must be mixed with an electron acceptor such as the methanofullerene PC₇₁BM, the composite films exhibited significant stiffness and brittleness. Use of processing additives such as DIO and PS, which can increase the efficiency of these devices, however, recovered some of the deformability. Substitution of PC₇₁BM with the small-molecule acceptor HPI-BT produced highly deformable films. While deformation in the elastic regime was easily rationalized by the presence of alkyl solubilizing groups, which are likely to

decrease the van der Waals attraction between adjacent molecules in the crystalline lattice, the mechanism of plastic deformation requires additional insights—perhaps in the form of molecular modeling and in situ X-ray diffraction—to understand. Regardless of the mechanism of deformation, however, it appears that the purported disadvantage of small-molecule semiconductors of mechanical fragility may not be as problematic as believed, especially because these films will be fabricated on and encapsulated in flexible foils that bear the load.

EXPERIMENTAL SECTION

Materials. 2,5-Di-(2-ethylhexyl)-3,6-bis(5"-*n*-hexyl-[2,2',5',2"]-terthiophen-5-yl)-pyrrolo[3,4-*c*]pyrrole-1,4-dione (SMDPPEH), 7,7'-[4,4-Bis(2-ethylhexyl)-4H-silolo[3,2-*b*:4,5-*b'*]dithiophene-2,6-diyl]bis-[6-fluoro-4-(5'-hexyl-[2,2'-bithiophen]-5-yl)benzo[*c*][1,2,5]-thiadiazole] (DTS(FBTTh₂)₂), 6,13-Bis(triisopropylsilyl)ethynyl-pentacene (TIPS-Pentacene), and 5,5'-(2,1,3-Benzothiadiazole-4,7-diyl)-2,1-ethenediyl]bis[2-hexyl-1*H*-isoin-dole-1,3(2*H*)-dione] (HPI-BT) were purchased from Sigma-Aldrich and used as received. 1,8-Diiodooctane (DIO) was purchased from Sigma-Aldrich with 98% purity. [6,6]-Phenyl C₇₁ butyric acid methyl ester (PC₇₁BM) technical grade was purchased from Solenne BV, Groningen, The Netherlands and used as received. Polystyrene samples of *M*_n = 900 kDa and 20 MDa were obtained from Alfa Aesar (Cat# 41943), Haverhill, MA and Pressure Chemical Co., Pittsburgh, PA., respectively. PDMS, Sylgard 184, Dow Corning, was prepared as stated in the manufacturer's instructions at a ratio of 10:1 (base:cross-linker) and cured at room temperature for 36–48 h when used for buckling and crack-onset experiments. (Tridecafluoro-1,1,2,2-tetrahydrooctyl)-1-tri-chlorosilane (FOTS) was obtained from Gelest. Poly(3,4-ethylenedioxythiophene) polystyrenesulfonate (PEDOT:PSS) (Clevios PH1000) was purchased from Heraeus. Dimethyl sulfoxide (DMSO) was purchased from BDH with purity of 99.9%. Zonyl (FS-300) fluorosurfactant, chloroform, acetone, and isopropanol were purchased from Alfa Aesar.

Preparation of Substrates. Glass slides used as substrates were cut into 2.5 cm squares with a diamond-tipped scribe. The slides were then successively cleaned with Alconox solution (2 mg mL⁻¹), deionized water, acetone, and isopropyl alcohol (IPA) in an ultrasonic bath for 10 min each and rinsed and dried with compressed air. After sonication, the glass was plasma treated at ~30 W for 3 min at a base pressure of 200 mTorr in ambient air to remove residual organic material and activate the surface. Silicon substrates used for AFM measurements were cut into 1 cm² pieces. To remove debris from the surface, the silicon substrates were cleaned and plasma treated in the same manner as described above.

PEDOT:PSS substrates were prepared from an aqueous solution containing 99 wt % Clevios PH 1000 and 1 wt % Zonyl fluorosurfactant. The solution was filtered with a 1 μ m glass microfiber (GMF) syringe before being spin coated onto glass for buckling measurements and PDMS for crack-onset measurements. For buckling experiments, PEDOT:PSS was annealed at 150 °C for 30 min in ambient air and allowed to naturally cool to room temperature. For crack-onset experiments PDMS was UV-ozone treated for 15 min prior to the spin-coating of PEDOT:PSS. After spin-coating, the films were dried under vacuum for 30 min, no thermal treatment.

Bilayer Film Buckling. The bilayer buckling technique is a modified version of the single-layer buckling test that has been employed by our group to determine the tensile moduli of especially brittle films that would otherwise fracture upon the release of prestrain in the single-layer buckling test. This method can also measure the tensile moduli of organic semiconductors that do not adhere to hydrophobic substrates. Bilayer buckling uses an interfacial layer of PEDOT:PSS, with a favorable surface energy, to permit the spin-coating and mechanical transfer of thin-films on hydrophobic substrates. The effective tensile modulus of each bilayer film was calculated using the same method as single layer buckling, eq 1.

$$\bar{E}_f = 3\bar{E}_s \left(\frac{\lambda}{2\pi h} \right)^3 \quad (1)$$

After obtaining the effective modulus of the bilayer film, E_{eff} , and measuring the tensile modulus of PEDOT:PSS in a separate buckle test, E_2 , we used eq 2 to extract the modulus of the small-molecule films, E_1 . Below, m is the modulus ratio, E_2/E_1 , and n is the thickness ratio, h_2/h_1 .

$$E_{\text{eff}} = \frac{1 + m^2 n^4 + 2mn(2n^2 + 3n + 2)}{(1 + n)^3(1 + mn)} E_1 \quad (2)$$

Preparation of Small-Molecule Solutions. Solutions of SMDPPEH, DTS(FBTTh₂)₂, TIPS-pentacene, HPI-BT, PC₇₁BM, and their physical blends were prepared in CHCl₃ (10 mg mL⁻¹) for the buckling technique, crack-onset tests, and AFM images. All solutions were stirred overnight at ambient temperature and for 2 h at 70 °C prior to spin-coating. The solutions were then filtered with a 1-μm GMF syringe filter immediately before being spin-coated onto glass, silicon, or PEDOT:PSS substrates.

Characterization of Materials. Atomic force microscopy (AFM) micrographs were taken using a Veeco Scanning Probe Microscope in tapping mode. Data were analyzed with Nanoscope Analysis v1.40 software (Bruker Corp.). The small-molecule solutions were spin-coated onto the silicon slides at a spin speed of 1000 rpm (500 rpm s⁻¹ ramp) for 120 s followed by 2000 rpm (1000 rpm s⁻¹ ramp) for 30 s. Afterward, spin-coating annealed samples were immediately placed in a nitrogen-filled glovebox and annealed at 70 °C for 10 min. After 10 min, the annealed samples were allowed to cool for 30 min on the hot plate.

■ ASSOCIATED CONTENT

■ Supporting Information

The Supporting Information is available free of charge on the ACS Publications website at DOI: 10.1021/acsami.6b02603.

Figures S1–S3, including photovoltaic characteristics of bulk heterojunction films, DSC thermograms, and UV–vis spectra (PDF)

■ AUTHOR INFORMATION

Corresponding Author

*E-mail: dlipomi@ucsd.edu (D.J.L.).

Notes

The authors declare no competing financial interest.

■ ACKNOWLEDGMENTS

This research was supported by the Air Force Office of Scientific Research (AFOSR) Young Investigator Program awarded to D.L., grant number FA9550-13-1-0156. D.R. and S.S. acknowledge support provided by the National Science Foundation Graduate Research Fellowship Program under Grant No. DGE-1144086 and the Kaplan Dissertation Year Fellowship, awarded to S.S., C.M.P., and T.-Q.N. thank the Office of Naval Research (Award # N000141410076). T.-Q.N. thanks the Camille Dreyfus Teacher-Scholar Awards Program.

■ REFERENCES

- (1) Li, Y.; Sonar, P.; Murphy, L.; Hong, W. High Mobility Diketopyrrolopyrrole (DPP)-Based Organic Semiconductor Materials for Organic Thin Film Transistors and Photovoltaics. *Energy Environ. Sci.* **2013**, *6*, 1684–1710.
- (2) Huang, Y.; Wen, W.; Mukherjee, S.; Ade, H.; Kramer, E. J.; Bazan, G. C. High-Molecular-Weight Insulating Polymers Can Improve the Performance of Molecular Solar Cells. *Adv. Mater.* **2014**, *26*, 4168–4172.

- (3) Love, J. A.; Proctor, C. M.; Liu, J.; Takacs, C. J.; Sharenko, A.; van der Poll, T. S.; Heeger, A. J.; Bazan, G. C.; Nguyen, T. Q. Film Morphology of High Efficiency Solution-Processed Small-Molecule Solar Cells. *Adv. Funct. Mater.* **2013**, *23*, 5019–5026.
- (4) Li, G.; Zhu, R.; Yang, Y. Polymer Solar Cells. *Nat. Photonics* **2012**, *6*, 153–161.
- (5) Savagatrup, S.; Rodriguez, D.; Printz, A. D.; Sieval, A. B.; Hummelen, J. C.; Lipomi, D. J. [70]PCBM and Incompletely Separated Grades of Methanofullerenes Produce Bulk Heterojunctions with Increased Robustness for Ultra-Flexible and Stretchable Electronics. *Chem. Mater.* **2015**, *27*, 3902–3911.
- (6) Carle, J. E.; Andersen, T. R.; Helgesen, M.; Bundgaard, E.; Jorgensen, M.; Krebs, F. C. A Laboratory Scale Approach to Polymer Solar Cells Using One Coating/Printing Machine, Flexible Substrates, No ITO, No Vacuum and No Spincoating. *Sol. Energy Mater. Sol. Cells* **2013**, *108*, 126–128.
- (7) Dupont, S. R.; Oliver, M.; Krebs, F. C.; Dauskardt, R. H. Interlayer Adhesion in Roll-to-Roll Processed Flexible Inverted Polymer Solar Cells. *Sol. Energy Mater. Sol. Cells* **2012**, *97*, 171–175.
- (8) Bruner, C.; Miller, N. C.; McGehee, M. D.; Dauskardt, R. H. Molecular Intercalation and Cohesion of Organic Bulk Heterojunction Photovoltaic Devices. *Adv. Funct. Mater.* **2013**, *23*, 2863–2871.
- (9) Savagatrup, S.; Printz, A. D.; Rodriguez, D.; Lipomi, D. J. Best of Both Worlds: Conjugated Polymers Exhibiting Good Photovoltaic Behavior and High Tensile Elasticity. *Macromolecules* **2014**, *47*, 1981–1992.
- (10) Awartani, O.; Lemanski, B. I.; Ro, H. W.; Richter, L. J.; DeLongchamp, D. M.; O'Connor, B. T. Correlating Stiffness, Ductility, and Morphology of Polymer:Fullerene Films for Solar Cell Applications. *Adv. Energy Mater.* **2013**, *3*, 399–406.
- (11) Kim, T.; Kim, J.-H.; Kang, T. E.; Lee, C.; Kang, H.; Shin, M.; Wang, C.; Ma, B.; Jeong, U.; Kim, T.-S.; Kim, B. J. Flexible, Highly Efficient All-Polymer Solar Cells. *Nat. Commun.* **2015**, *6*, 8547.
- (12) Wu, H.-C.; Benight, S. J.; Chortos, A.; Lee, W.-Y.; Mei, J.; To, J. W. F.; Lu, C.; He, M.; Tok, J. B.-H.; Chen, W.-C.; Bao, Z. A Rapid and Facile Soft Contact Lamination Method: Evaluation of Polymer Semiconductors for Stretchable Transistors. *Chem. Mater.* **2014**, *26*, 4544–4551.
- (13) Liang, J.; Li, L.; Chen, D.; Hajagos, T.; Ren, Z.; Chou, S.-Y.; Hu, W.; Pei, Q. Intrinsically Stretchable and Transparent Thin-Film Transistors Based on Printable Silver Nanowires, Carbon Nanotubes and an Elastomeric Dielectric. *Nat. Commun.* **2015**, *6*, 7647.
- (14) Tahk, D.; Lee, H. H.; Khang, D.-Y. Elastic Moduli of Organic Electronic Materials by the Buckling Method. *Macromolecules* **2009**, *42*, 7079–7083.
- (15) Lin, Y.; Li, Y.; Zhan, X. Small Molecule Semiconductors for High-Efficiency Organic Photovoltaics. *Chem. Soc. Rev.* **2012**, *41*, 4245–4272.
- (16) Printz, A. D.; Savagatrup, S.; Rodriguez, D.; Lipomi, D. J. Role of Molecular Mixing on the Stiffness of Polymer:fullerene Bulk Heterojunction Films. *Sol. Energy Mater. Sol. Cells* **2015**, *134*, 64–72.
- (17) O'Connor, B.; Chan, E. P.; Chan, C.; Conrad, B. R.; Richter, L. J.; Kline, R. J.; Heeney, M.; McCulloch, I.; Soles, C. L.; DeLongchamp, D. M. Correlations between Mechanical and Electrical Properties of Polythiophenes. *ACS Nano* **2010**, *4*, 7538–7544.
- (18) Printz, A. D.; Zaretski, A. V.; Savagatrup, S.; Chiang, A. S.-C.; Lipomi, D. J. Yield Point of Semiconducting Polymer Films on Stretchable Substrates Determined by Onset of Buckling. *ACS Appl. Mater. Interfaces* **2015**, *7*, 23257–23264.
- (19) Tamayo, A.; Kent, T.; Tantitiwat, M.; Dante, M. a.; Rogers, J.; Nguyen, T.-Q. Influence of Alkyl Substituents and Thermal Annealing on the Film Morphology and Performance of Solution Processed, Diketopyrrolopyrrole-Based Bulk Heterojunction Solar Cells. *Energy Environ. Sci.* **2009**, *2*, 1180–1186.
- (20) Cheng, Y. J.; Liao, M. H.; Chang, C. Y.; Kao, W. S.; Wu, C. E.; Hsu, C. S. Di(4-Methylphenyl)methano-C60 Bis-Adduct for Efficient and Stable Organic Photovoltaics with Enhanced Open-Circuit Voltage. *Chem. Mater.* **2011**, *23*, 4056–4062.

- (21) Simmons, G. W. H. *Single Crystal Elastic Constants and Calculated Aggregate Properties: A Handbook*; The MIT Press: Cambridge, 1971.
- (22) Giri, G.; Verploegen, E.; Mannsfeld, S. C. B.; Atahan-Evrenk, S.; Kim, D. H.; Lee, S. Y.; Becerril, H. a.; Aspuru-Guzik, A.; Toney, M. F.; Bao, Z. Tuning Charge Transport in Solution-Sheared Organic Semiconductors Using Lattice Strain. *Nature* **2011**, *480*, 504–508.
- (23) van der Poll, T. S.; Love, J. a.; Nguyen, T.-Q.; Bazan, G. C. Non-Basic High-Performance Molecules for Solution-Processed Organic Solar Cells. *Adv. Mater.* **2012**, *24*, 3646–3649.
- (24) Tamayo, A. B.; Dang, X. D.; Walker, B.; Seo, J.; Kent, T.; Nguyen, T.-Q. A Low Band Gap, Solution Processable Oligothiophene with a Dialkylated Diketopyrrolopyrrole Chromophore for Use in Bulk Heterojunction Solar Cells. *Appl. Phys. Lett.* **2009**, *94*, 1–3.
- (25) Anctil, A.; Babbitt, C. W.; Raffaele, R. P.; Landi, B. J. Material and Energy Intensity of Fullerene Production. *Environ. Sci. Technol.* **2011**, *45*, 2353–2359.
- (26) Nielsen, C. B.; Holliday, S.; Chen, H.; Cryer, S. J.; McCulloch, I. Non-Fullerene Electron Acceptors for Use in Organic Solar Cells. *Acc. Chem. Res.* **2015**, *48*, 2803–2812.
- (27) Peet, J.; Kim, J. Y.; Coates, N. E.; Ma, W. L.; Moses, D.; Heeger, A. J.; Bazan, G. C. Efficiency Enhancement in Low-Bandgap Polymer Solar Cells by Processing with Alkane Dithiols. *Nat. Mater.* **2007**, *6*, 497–500.
- (28) Chung, J. Y.; Nolte, A. J.; Stafford, C. M. Surface Wrinkling: A Versatile Platform for Measuring Thin-Film Properties. *Adv. Mater.* **2011**, *23*, 349–368.
- (29) Savagatrup, S.; Makaram, A. S.; Burke, D. J.; Lipomi, D. J. Mechanical Properties of Conjugated Polymers and Polymer-Fullerene Composites as a Function of Molecular Structure. *Adv. Funct. Mater.* **2014**, *24*, 1169–1181.
- (30) Park, B. S.-I.; Ahn, J.; Feng, X.; Wang, S.; Huang, Y.; Rogers, J. A. Theoretical and Experimental Studies of Bending of Inorganic Electronic Materials on Plastic Substrates **. *Adv. Funct. Mater.* **2008**, *18*, 2673–2684.
- (31) Hopkinson, P. E.; Staniec, P. A.; Pearson, A. J.; Dunbar, A. D. F.; Wang, T.; Ryan, A. J.; Jones, R. A. L.; Lidzey, D. G.; Donald, A. M. A Phase Diagram of the P3HT:PCBM Organic Photovoltaic System: Implications for Device Processing and Performance. *Macromolecules* **2011**, *44*, 2908–2917.
- (32) Postema, A. R.; Liou, K.; Wudl, F.; Smith, P. Highly Oriented, Low-Modulus Materials from Liquid Crystalline Polymers: The Ultimate Penalty for Solubilizing Alkyl Side Chains. *Macromolecules* **1990**, *23*, 1842–1845.
- (33) Zhao, J.; Swinnen, A.; Van Assche, G.; Manca, J.; Vanderzande, D.; Van Mele, B. Phase Diagram of P3HT/PCBM Blends and Its Implication for the Stability of Morphology. *J. Phys. Chem. B* **2009**, *113*, 1587–1591.
- (34) Cun, H.; Wang, Y.; Du, S.; Zhang, L.; Zhang, L.; Yang, B.; He, X.; Wang, Y.; Zhu, X.; Yuan, Q.; Zhao, Y.-P.; Ouyang, M.; Hofer, W. A.; Pennycook, S. J.; Gao, H. Tuning Structural and Mechanical Properties of Two-Dimensional Molecular Crystals: The Roles of Carbon Side Chains. *Nano Lett.* **2012**, *12*, 1229–1234.
- (35) Sharenko, A.; Kuik, M.; Toney, M. F.; Nguyen, T.-Q. Crystallization-Induced Phase Separation in Solution-Processed Small Molecule Bulk Heterojunction Organic Solar Cells. *Adv. Funct. Mater.* **2014**, *24*, 3543–3550.
- (36) Savagatrup, S.; Printz, A. D.; O'Connor, T. F.; Zaretski, A. V.; Rodriguez, D.; Sawyer, E. J.; Rajan, K. M.; Acosta, R. I.; Root, S. E.; Lipomi, D. J. Mechanical Degradation and Stability of Organic Solar Cells: Molecular and Microstructural Determinants. *Energy Environ. Sci.* **2015**, *8*, 55–80.
- (37) Perez, L. A.; Chou, K. W.; Love, J. A.; van der Poll, T. S.; Smilgies, D. M.; Nguyen, T.-Q.; Kramer, E. J.; Amassian, A.; Bazan, G. C. Solvent Additive Effects on Small Molecule Crystallization in Bulk Heterojunction Solar Cells Probed during Spin Casting. *Adv. Mater.* **2013**, *25*, 6380–6384.
- (38) McDowell, C.; Abdelsamie, M.; Zhao, K.; Smilgies, D.-M.; Bazan, G. C.; Amassian, A. Synergistic Impact of Solvent and Polymer Additives on the Film Formation of Small Molecule Blend Films for Bulk Heterojunction Solar Cells. *Adv. Energy Mater.* **2015**, *5*, 1–9.